Chapter 4: Turbulence at Small Scales

Part 6: 1D Spatial and Time Series Spectra

We have already noted the following:

1. Most often spectra are obtained from single point time series measurements and transformed to 1D spatial spectra via Taylors frozen turbulence hypothesis; or in some cases 1D spatial measurements along a line.

2. In either case, the relations between 1D and 3D spectra have shown that the Kolmogorov hypotheses are valid not only for 3D spectra as originally hypothesized, but also for their 1D counterpart.

Herein, we review several techniques for obtaining 1D spectra:

1. Temporal using autocorrelation $f(t)$ (or convolution integral) and Taylor hypotheses.
2. Spatial using even autocorrelation $f(r)$ and homogeneous isotropic turbulence assumptions.
3. Spatial using odd autocorrelation $f(r)$ and nonhomogeneous non-isotropic assumptions.

Prior to reviewing the techniques for obtaining 1D spectra, power law and model spectrums are discussed, as these will be used in analyzing the 1D spectra and their 3D counterparts using Kolmogorov scaling. Subsequently in Part 7, the 1D and 3D spectra will be further analyzed using alternate scaling such as compensated spectra, etc.

Power-law spectra

Chapter 4 Parts 0 and 4 already introduced Kolmogorov hypotheses and resulting spectra based on dimensional analysis and its relationship to power law spectra. In the inertial subrange, the power law spectra are of the form

$$E_{11}(\kappa_1) = C_1 A \kappa_1{}^{-p} \quad (1)$$

Where C_1 is a constant and A is a normalization factor, e.g., $A = \overline{u_1^2} L_{11}^{1-p}$, i.e., same units as $\varepsilon^{2/3}$. If $E_{11}(\kappa_1)$ is given by (1), then using $E(k) = f\big(E_{11}(\kappa_1)\big)$ derived in Part 5, it follows that.

$$E(\kappa) = CA\kappa^{-p}$$

Where $C = \frac{1}{2}p(2+p)C_1$.

Proof in Appendix A.1

Similarly, for E_{22}

$$E_{22}(\kappa) = C_1{}' A \kappa^{-p}$$

Where $C_1{}' = \frac{1}{2}(1+p)C_1$.

Proof in Appendix A.2

Thus, the power-law exponent p is the same for the three spectra and the constants $C, C_1, C_1{}'$ are related.

Recall, in the inertial subrange based on dimensional analysis

$$E(\kappa) = C\varepsilon^{2/3}\kappa^{-5/3}$$

Where $C \sim 1.5$ (from experiments).

Therefore, for E_{11} and E_{22}

$$E_{11}(\kappa_1) = C_1\varepsilon^{2/3}{\kappa_1}^{-5/3} \qquad \boxed{C_1 = \frac{18}{55}C = 0.49}$$

$$E_{22}(\kappa_1) = {C_1}'\varepsilon^{2/3}{\kappa_1}^{-5/3} \qquad \boxed{C_1' = \frac{4}{3}C_1 = \frac{24}{55}C = 0.65}$$

A model spectrum

An analytical model spectrum is used for the evaluation of the Kolmogorov hypotheses and the experimentally (or numerically) obtained spectrums:

$$E(\kappa) = C\varepsilon^{2/3}\kappa^{-5/3}f_L(\kappa L)f_\eta(\kappa\eta) \quad (2)$$

Where f_L and f_η are specified non-dimensional functions. The function f_L determines the shape of the energy-containing range, $f_L \to 1$ for $\kappa L \to \infty$, i.e., small $l = 2\pi/\kappa$. The function f_η determines the shape of the dissipation range, $f_\eta \to 1$ for $\kappa\eta \to 0$, i.e., large $l = 2\pi/\kappa$.

In the inertial subrange, both f_L and $f_\eta \to 1$ so that the Kolmogorov -5/3 spectrum is obtained with the constant C recovered.

The specification of f_L is

$$f_L(\kappa L) = \left(\frac{\kappa L}{[(\kappa L)^2 + c_L]^{\frac{1}{2}}} \right)^{\frac{5}{3}+p_0} \qquad (3)$$

p_0 is taken to be 2, and c_L is a positive constant. Clearly, $f_L \to 1$ for large κL, while the exponent $\frac{5}{3} + p_0$ leads to $E(\kappa) \propto \kappa^{p_0} = \kappa^2$ for small κL. Or for $p_0 = 4$ leads to $E(\kappa) \propto \kappa^4$ for small κL.

The specification of f_η is

$$f_\eta(\kappa\eta) = exp\left\{-\beta\left\{\left[(\kappa\eta)^4 + {c_\eta}^4\right]^{1/4} - c_\eta\right\}\right\} \qquad (4)$$

Where β and c_η are positive constants. For $c_\eta = 0$: $f_\eta(\kappa\eta) = \exp(-\beta\kappa\eta)$. In either case, exponential decay is exhibited for large $\kappa\eta$.

Since the velocity field $\underline{u}(\underline{x})$ is infinitely differentiable, for large κ, the energy spectrum decays more rapidly than any power of κ, thus, exponential decay is used, as suggested by Kraichnan. Experiments support exponential decay with $\beta = 5.2$. However, the simplified exponential form with $c_\eta = 0$ departs from unity too rapidly for small $\kappa\eta$ and the value of β is constrained to be $\beta = 2.1$. These deficiencies are remedied by Eq. (4).

For specified values of k, ε, and v, the model spectrum is determined using Eq. (2), (3) and (4) with $C = 1.5$ and $\beta = 5.2$. Alternatively, the non-dimensional model spectrum is uniquely determined by a specified value of R_λ.

c_L and c_η are determined by the requirement that $E(\kappa)$ and $2\nu\kappa^2 E(\kappa)$ integrate to k and ε, respectively: at high Re their values are $c_L \approx 6.78$ and $c_\eta \approx 0.40$.

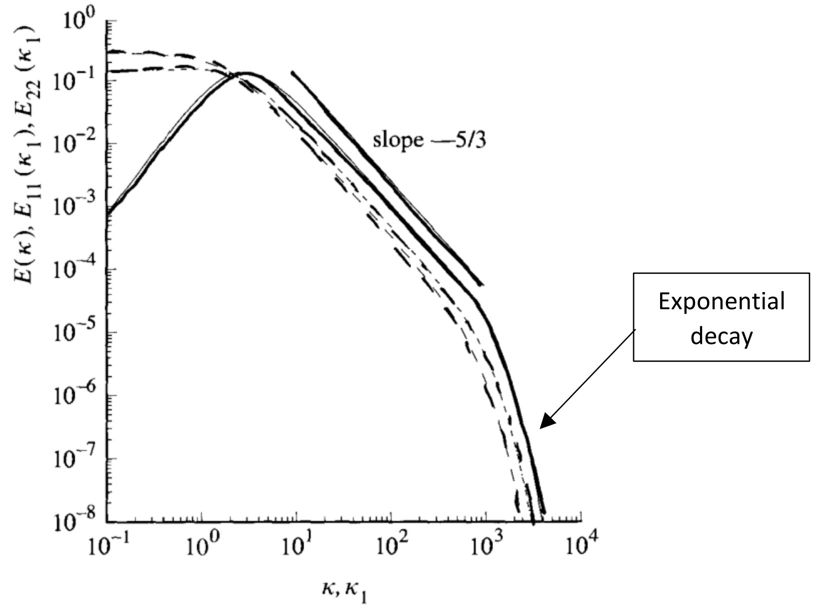

Fig. 6.11. Comparison of spectra in isotropic turbulence at $R_\lambda = 500$: solid line, $E(\kappa)$; dashed line, $E_{11}(\kappa_1)$; dot-dashed line, $E_{22}(\kappa_1)$. From the model spectrum, Eq. (6.246). (Arbitrary units.)

Fig. 6.11 shows $E(\kappa), E_{11}(\kappa)$ and $E_{22}(\kappa)$ at $R_\lambda = 500$. In the inertial subrange, all spectra exhibit power-law behavior with $p = 5/3$, and their ratio is given by the ratio of C, C_1, C_1'.

At low wave number $E(\kappa) \to 0$ as κ^2, while one-dimensional spectra are maximum at $\kappa = 0$, which shows the effects of aliasing, i.e., the fact that the 1D specta contain contributions from $\kappa > \kappa_1$. Also, at low wave number

$$E_{11} = 2E_{22}$$

in accordance with the ratios of integral scales L_{11} and L_{22}, i.e., $L_{22} = L_{11}/2$.

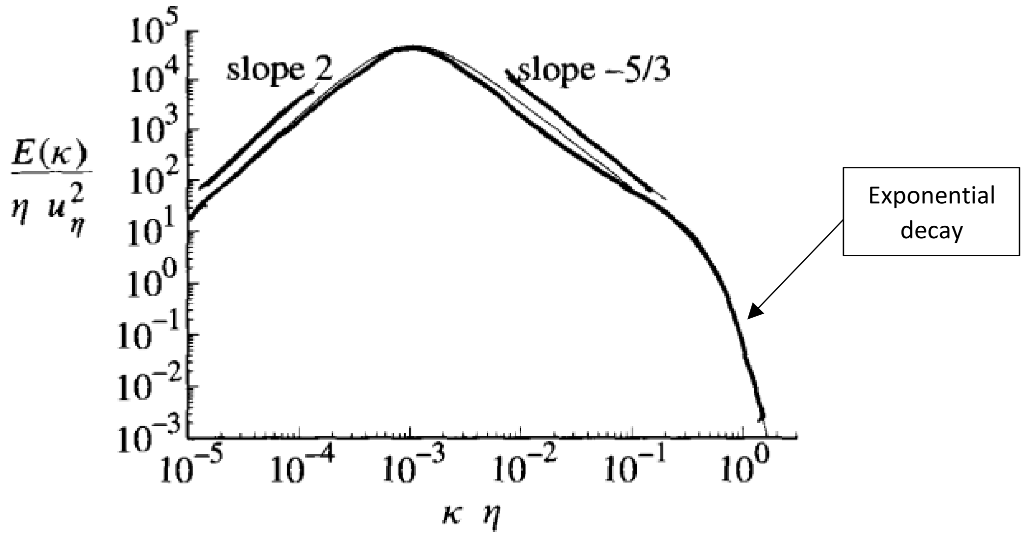

Fig. 6.13. The model spectrum (Eq. (6.246)) for $R_\lambda = 500$ normalized by the Kolmogorov scales.

Fig. 6.13 is a log-log plot of the model spectrum (with Kolmogorov scaling) for $R_\lambda = 500$. The power laws $E(\kappa) \sim \kappa^2$ at low wave number and $E(\kappa) \sim \kappa^{-5/3}$ in the inertial subrange are shown, as is the exponential decay at large κ.

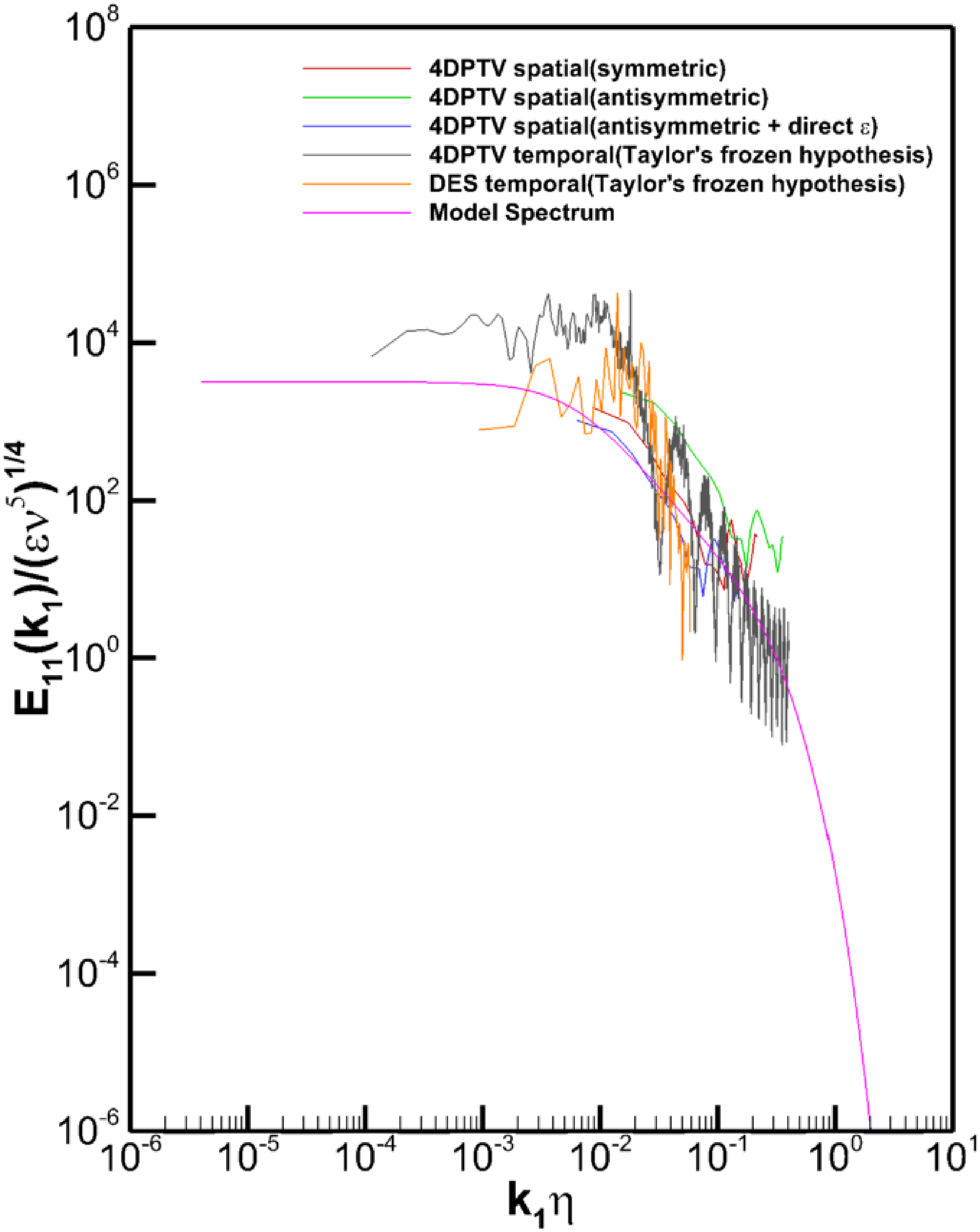

Yugo Sanada, Zachary Starman, Shanti Bhushan and Frederick Stern. Measurements of 3D Vortex Onset and Progression for 5415 Straight Ahead, Static Drift and Pure Sway, Appendix A. Turbulence Analysis of SDVP for β=10° at x/L=0.12.

Techniques for obtaining 1D spectra

Method 1: Energy Spectrum from spatial autocorrelation $\boldsymbol{f(r)}$: even

1. Calculate symmetric spatial autocorrelation function.

$$f(r) = \frac{\overline{u(x)u(x+r)}}{\overline{u^2}}$$

2. Obtain 1D energy spectrum from Fourier transform of $f(r)$

$$E_{11}(\kappa) = \frac{2}{\pi}\overline{u^2}\int_0^{\infty} f(r_1)\cos(\kappa_1 r_1)d\,r_1$$

3. Calculate the Taylor microscale and integral length scale.

$$\lambda_f = [-2/f''(0)]^{1/2}, \qquad \Lambda_f = \frac{1}{2}\int_{-\infty}^{\infty} f(r)dr = \int_0^{\infty} f(r)dr$$

4. Calculate dissipation.

$$\varepsilon = 30\nu\frac{\overline{u^2}}{\lambda_f^2}$$

5. Calculate Kolmogorov scale.

$$\eta = \left(\frac{\nu^3}{\varepsilon}\right)^{1/4}$$

6. Plot $E_{11}(\kappa_1)/(\varepsilon\nu^5)^{1/4}$ vs $\kappa_1\eta$

Method 2: Energy Spectrum from spatial autocorrelation $f(r)$: odd

1. Calculate the antisymmetric spatial autocorrelation function.

$$f(\pm r) = \frac{\overline{u(x)u(x \pm r)}}{\overline{u^2}}$$

2. Obtain 1D energy spectrum in space from Fourier transform of $f(r)$

$$E_{11}(\kappa) = \frac{\overline{u^2}}{\pi} \int_{-\infty}^{\infty} f(r_1) \cos(\kappa_1 r_1) d\, r_1$$

3. Calculate the Taylor microscale and integral length scale.

$$\lambda_f = \frac{\left[-f'(0) + [\{f'(0)\}^2 - 2f''(0)]^{\frac{1}{2}}\right]}{f''(0)}, \qquad \Lambda_f = \frac{1}{2} \int_{-\infty}^{\infty} f(r) dr$$

4. Calculate dissipation.

$$\varepsilon = \upsilon \left(\overline{u_{i,j} u_{i,j}} + \frac{\partial^2 \overline{u_i u_j}}{\partial x_i \partial x_j} \right)$$

5. Calculate Kolmogorov scale.

$$\eta = \left(\frac{\nu^3}{\varepsilon} \right)^{1/4}$$

6. Plot $E_{11}(\kappa_1)/(\varepsilon \nu^5)^{1/4}$ vs $\kappa_1 \eta$

Method 3: Energy spectrum from temporal autocorrelation $f(\tau)$

1. Calculate temporal autocorrelation.

$$R_E(\tau) = \frac{\overline{u(t)u(t+\tau)}}{\overline{u^2}}$$

2. Obtain Fourier transform of $R_E(\tau)$.

$$\hat{R}_E(2\pi\omega) = 2\int_0^\infty R_E(\tau)\cos(2\pi\omega\tau)\,d\tau$$

(Note: ω : Frequency [Hz])

3. Calculate the time micro and integral scales.

$$\tau_E = [-2/f''(0)]^{1/2}, \qquad T = \int_0^\infty f(\tau)d\tau$$

4. Using Taylor hypothesis, calculate the Taylor microscale, dissipation, and Kolmogorov scale.

$$\lambda_f = \overline{U}\tau_E, \qquad \varepsilon = 30\nu\frac{\overline{u^2}}{\lambda_f^2}, \qquad \eta = \left(\frac{\nu^3}{\varepsilon}\right)^{1/4}$$

5. Calculate the 1D energy spectrum in time from the Fourier transform of $R_E(\tau)$.

$$\hat{E}_{11}(\omega) = 2\overline{u^2}\hat{R}_E(2\pi\omega)$$

6. Calculate the 1D energy spectrum in space from the 1D energy spectrum in time.

$$E_{11}(\kappa_1) = \frac{\overline{U}}{2\pi}\hat{E}_{11}(\omega)$$

7. Plot $E_{11}(\kappa_1)/(\varepsilon\nu^5)^{1/4}$ vs $\kappa_1\eta$

Details Method 3

Taylor's frozen turbulence hypothesis relates time sequence of streamwise velocity data to data distributed along a straight line in the flow direction as if the turbulent velocity field at a given instant in time convects downstream at the local mean velocity, i.e., as if it were frozen.

$$u(x, t+\tau) = u\left(x - \overline{U}\tau, t\right) \quad (1)$$

Where $x - \overline{U}\tau$ represents the upstream point, so that

$$\overline{u(x,t)u(x,t+\tau)} = \overline{u(x,t)u(x-\overline{U}\tau,t)} \quad (2)$$

Combining with $f(r)$ and $R_E(\tau)$ definitions

$$f(r) = \frac{\overline{u(x)u(x+r)}}{\overline{u^2(x)}} \quad (3)$$

$$R_E(\tau) = \frac{\overline{u(t)u(t+\tau)}}{\overline{u^2}} \quad (4)$$

Taking $r = -\overline{U}\tau$ in Eq. (3)

$$f\left(-\overline{U}\tau\right) = \frac{\overline{u(x)u\left(x-\overline{U}\tau\right)}}{\overline{u^2(x)}}$$

Comparing with Eq. (4) and adding t dependence to Eq. (3) and x dependence to Eq. (4)

$$\underbrace{\frac{\overline{u(x,t)u(x,t+\tau)}}{\overline{u^2}}}_{R_E(\tau)} = \underbrace{\frac{\overline{u(x,t)u\left(x-\overline{U}\tau,t\right)}}{\overline{u^2}}}_{f\left(-\overline{U}\tau\right)} \quad (5)$$

Assuming zero separation $(x + r = 0,)$ and zero time-delay $(t + \tau = 0)$ and using the symmetry of $R_E(\tau)$ and $f(r)$ yields

$$x = \pm r, \qquad t = \pm\tau$$

Using these relations in Eqs. (3) and (4), including their t and x dependence

$$f(r = x) = \frac{\overline{u(x,t)u(0,t)}}{\overline{u^2}} \quad (6)$$

$$R_E(\tau = t) = \frac{\overline{u(x,t)u(x,0)}}{\overline{u^2}} \quad (7)$$

Comparing the RHS of Eq. (5) and (6), shows that

$$x = \overline{U}\tau \Rightarrow \tau = \frac{x}{\overline{U}} \quad (8)$$

Substituting Eq. (8) into (7) and equating to (6) yields

$$R_E\left(\tau = t = \frac{x}{\overline{U}}\right) = \frac{\overline{u\left(x, \frac{x}{\overline{U}}\right)u(x,0)}}{\overline{u^2}} = f(r = x) = \frac{\overline{u(x,t)u(0,t)}}{\overline{u^2}}$$

$$R_E\left(\frac{x}{\overline{U}}\right) = f(x)$$

Using the definitions of $E_{11}(k_1)$ and $\hat{R}_E(\omega')$

$$E_{11}(k_1) = \frac{\overline{u^2}}{\pi}\int_{-\infty}^{\infty} e^{-ik_1 x} f(x)dx \qquad \hat{R}_E(\omega') = \int_{-\infty}^{\infty} e^{-i\tau\omega'} R_E(\tau)d\tau \qquad \boxed{\omega' = 2\pi\omega}$$

$$\boxed{f(x) = R_E\left(\frac{x}{\overline{U}}\right)}$$

$$= \frac{\overline{u^2}}{\pi}\int_{-\infty}^{\infty} e^{-ik_1 x} R_E\left(\frac{x}{\overline{U}}\right)dx$$

$$\boxed{dx = \overline{U}d\tau}$$

$$= \frac{\overline{u^2}}{\pi}\int_{-\infty}^{\infty} e^{-ik_1\overline{U}\tau} R_E(\tau)\overline{U}d\tau$$

From the comparison of the exponentials highlighted in yellow, the following relationship is obtained:

$$k_1\overline{U}\tau = 2\pi\omega\tau \;\Rightarrow \omega = k_1\overline{U}/2\pi.$$

$$= \frac{\overline{u^2}\,\overline{U}}{\pi}\int_{-\infty}^{\infty} e^{-i\tau\omega'} R_E(\tau)d\tau = \frac{\overline{u^2}\,\overline{U}}{\pi}\hat{R}_E(\omega') \quad (9)$$

Recall (Chapter 2)

$$\hat{E}_{11}(\omega) = 2\overline{u^2}\hat{R}_E(2\pi\omega) \quad (10)$$

Combining Eqs. (9) and (10), obtain a relation between $\hat{E}_{11}(\omega)$ and $E_{11}(k_1)$:

$$E_{11}(k_1) = \frac{\overline{u^2}\,\overline{U}}{\pi}\frac{\hat{E}_{11}(\omega)}{2\overline{u^2}} = \frac{\overline{U}}{2\pi}\hat{E}_{11}(\omega)$$

Or equivalently

$$\hat{E}_{11}(\omega) = \frac{2\pi}{\overline{U}}E_{11}\left(\frac{2\pi\omega}{\overline{U}}\right)$$

Thus, $E_{11}(k_1)$ can be determined from measurements of $\hat{E}_{11}(\omega) = \hat{E}_{11}\left(\frac{k_1\overline{U}}{2\pi}\right)$.
Measured time spectra via Taylor hypothesis provide $E_{11}(k_1)$

Taylor micro-scale

$$f(x) = R_E\left(\tau = \frac{x}{\overline{U}}\right)$$

$$f' = R_{E,\tau}\frac{d\tau}{dx} = R_E{}'/\overline{U}$$

$$f'' = R_E{}''/\overline{U}^2$$

$$\lambda_f{}^2 = -\frac{2}{f''} = -\frac{2\overline{U}^2}{R_E{}''} = \overline{U}^2\lambda_t{}^2$$

Taylor macro-scale

$$\Lambda_f = \int_0^\infty f(x)dx$$

$$= \int_0^\infty R_E(\tau)\,\overline{U}d\tau$$

$$\Lambda_f = \overline{U}\Lambda_t$$

Method 4: Energy spectrum from Fourier Transform of the time auto-correlation coefficient $R_E(\tau)$

Alternative derivation using definition of convolution in Appendix A.3

1. Definition of $R_E(\tau)$

$$R_E(\tau) = \frac{\overline{u(t)u(t+\tau)}}{\overline{u^2}} = \frac{1}{\overline{u^2}} \lim_{T\to\infty} \frac{1}{2T} \int_{-T}^{T} u(t)u(t+\tau)dt$$

2. Fourier transform of $R_E(\tau)$

$$\mathcal{F}\{R_E(\tau)\} = \hat{R}_E(\omega') = \int_{-\infty}^{\infty} \left[\frac{1}{\overline{u^2}} \lim_{T\to\infty} \frac{1}{2T} \int_{-T}^{T} u(t)u(t+\tau)dt\right] e^{-i\omega'\tau} d\tau$$

$$\hat{R}_E(\omega') = \frac{1}{\overline{u^2}} \lim_{T\to\infty} \frac{1}{2T} \int_{-T}^{T} u(t)e^{i\omega' t}dt \int_{-\infty}^{\infty} u(t+\tau)\, e^{-i\omega'(\tau+t)} d\tau$$

3. Change of variable: $s = \tau + t,\, ds = d\tau$

$$\hat{R}_E(\omega') = \frac{1}{\overline{u^2}} \lim_{T\to\infty} \frac{1}{2T} \underbrace{\int_{-T}^{T} u(t)e^{i\omega' t}dt}_{\boxed{\hat{u}^*(\omega)}} \underbrace{\int_{-\infty}^{\infty} u(s)e^{-i\omega' s} ds}_{\boxed{\hat{u}(\omega)}}$$

4. Definition of $\hat{E}_{11}(\omega)$

$$\hat{R}_E(\omega') = \frac{1}{\overline{u^2}} \lim_{T\to\infty} \frac{1}{2T}\, \hat{u}(\omega)\hat{u}^*(\omega) = \frac{1}{\overline{u^2}} \lim_{T\to\infty} \frac{1}{2T} |\hat{u}(\omega)|^2 \equiv \frac{\hat{E}_{11}(\omega)}{2\overline{u^2}}$$

Where the following definition was used

$$\lim_{T\to\infty}\frac{1}{T}|\hat{u}(\omega)|^2 \equiv \hat{E}_{11}(\omega)$$

And the limit is evaluated numerically based on time series interval $u(t)$ used to obtain $\mathcal{F}\{u(t)\}$ either experimentally or DES.

Solving for $\hat{E}_{11}(\omega)$ yields

$$\hat{E}_{11}(\omega) = 2\overline{u^2}\hat{R}_E(\omega')$$

5. Calculate the 1D energy spectrum in space from the 1D energy spectrum in time.

$$E_{11}(\kappa_1) = \frac{\overline{U}}{2\pi}\hat{E}_{11}(\omega)$$

6. Plot $E_{11}(\kappa_1)/(\varepsilon\nu^5)^{1/4}$ vs $\kappa_1\eta$

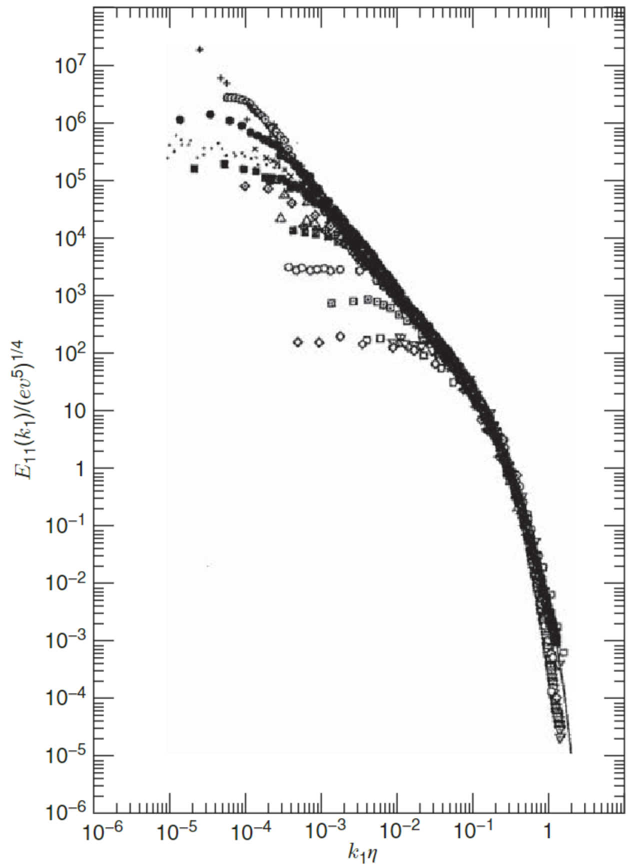

Figure 4.7 Experimental tests of the −5/3 law [3]. Reprinted with the permission of Cambridge University Press.

$$E(k) = (\varepsilon \nu^5)^{1/4}\varphi(k\eta) = \eta {u_\eta}^2 \varphi(k\eta)$$

$\varphi(k\eta) =$ *Kolmogorov spectrum function*.

Measured spectra clearly show the universal equilibrium range and inertial subrange Kolmogorov -5/3 spectrum, which extends over several decades of wave number. The extent of the inertial subrange increases with R_λ. Data show $C_1 \sim .5$ such that $C \sim 1.4$. Recent estimates $Re_\lambda = 1000, C = 1.58$.

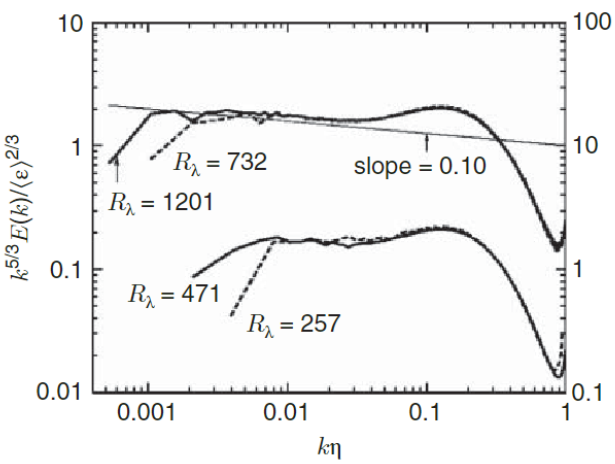

Figure 4.8 Compensated energy spectrum as given in [21]. With increasing R_λ the simulations used 512^3, 1024^3, 2048^3, and 4096^3 meshes. Scales on the left and right are for the upper and lower curves, respectively. Reproduced from *Physics of Fluids*, Vol. 15, pp. L21–L24, 2003, with the permission of AIP Publishing.

Compensated spectrum $E(k)/\varepsilon^{2/3}{k_1}^{-5/3}$ for $R_\lambda = 1201$ DNS should be constant, but small negative slope $\sim .1$ suggests that a more appropriate spectrum for the inertial range might be $\sim k^{-\frac{5}{3}-0.1}$.

This plot also shows the *bottleneck effect,* which is represented by the pronounced peak that is formed for wave numbers just larger than those in the inertial range. One explanation for this phenomenon is that in this range there is insufficient small-scale vortices to efficiently dissipate energy so that it accumulates to form a bump. This effect vanishes for high Re.

One explanation for the departure of small-scale turbulence from the -5/3 law is the fact that ε is highly intermittent in space and time.

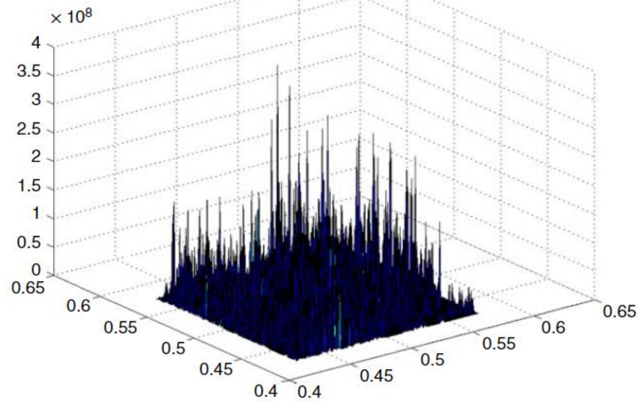

Figure 4.9 Dissipation rate on a plane showing intermittency within a region of isotropic turbulence computed in a vortex filament simulation of flow in a periodic box.

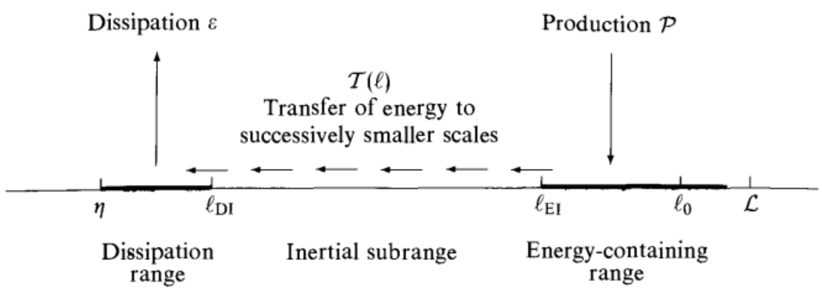

Fig. 6.2. A schematic diagram of the energy cascade at very high Reynolds number.

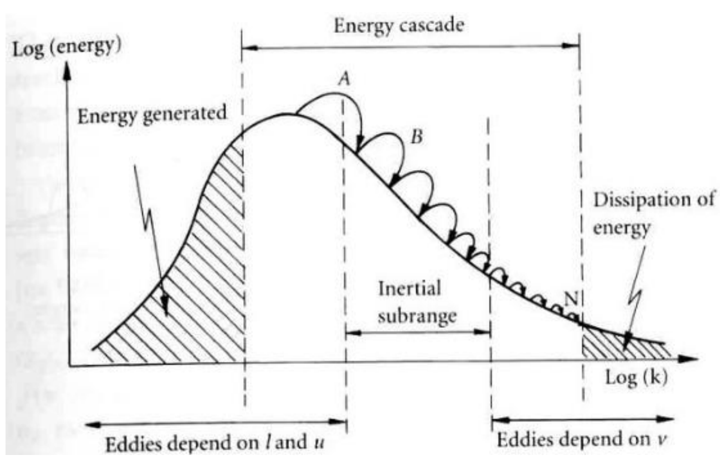

Clearly Kolmogorov -5/3 spectrum fully supports important turbulence concepts of Richardson cascade, Kolmogorov hypotheses, theory of isotropic turbulence and dimensional analysis; albeit with issues of backscatter suggesting energy transfer is a two-way equilibrium process including intermittency of dissipation.

Taylor Frozen Turbulence Hypothesis

For small Δt, assume turbulence frozen as it convects past probe at x such that changes $U_i(t) \propto$ changes $U_i(x)$, i.e.,

$$\frac{dU_i}{dx} = -\frac{1}{U_c}\frac{dU_i}{dt}$$

Where $U_c =$ convection velocity of frozen turbulence.

Requires assumption $\underline{a} = 0$ at x (i.e., pressure and viscous forces =0)

$$\frac{\partial U_i}{\partial t} + U_1\frac{\partial U_i}{\partial x} + U_2\frac{\partial U_i}{\partial y} + U_3\frac{\partial U_i}{\partial z} = 0 \qquad \boxed{U_c = U_1}$$

That is, for the last 2 terms $= 0$ [i.e., 1-axis is aligned with the direction of the mean flow $U_i = (U_1, 0, 0)$]

$$\frac{dU_i}{dx} = -\frac{1}{U_c}\frac{dU_i}{dt}$$

Must be far from boundaries and other sources $\nabla P + \nabla^2\underline{u}$. More detailed analysis shows that actual requirement is that: $\sqrt{\langle u_i u_i\rangle}/U_1 \ll 1$, $p \sim u_1^2$, and Re large enough viscous effects negligible (Kundu et al. Ex. 12.11). Also see Pope pp. 223-224.

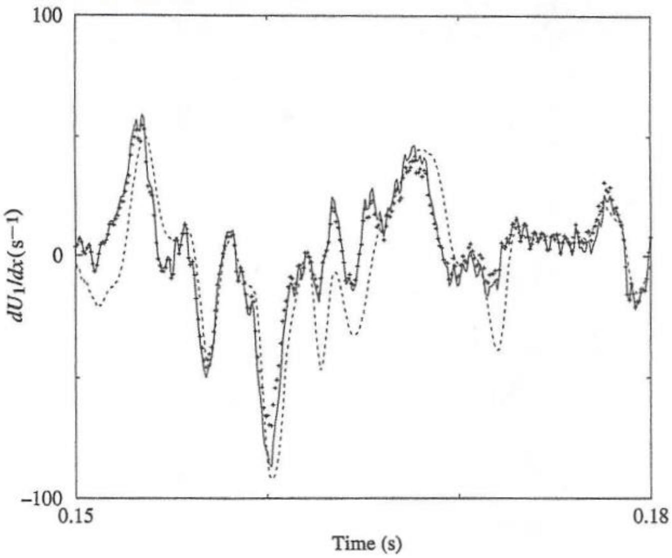

Fig. 3.5 Comparison of time-series signals determined from Taylor's hypothesis [Eqs. (3.30) —— and (3.32) +++] and from the continuity equation (···) using mixing-layer data from a 12-sensor probe. (From [31].)

Continuity:

$$\frac{\partial U_1}{\partial x} = -\left(\frac{\partial U_2}{\partial y} + \frac{\partial U_3}{\partial z}\right)$$

Reasonable agreement channel flow above buffer layer. Used to transform 1D f spectra to streamwise k spectra:

$$k_x \approx \frac{2\pi f}{U_1}$$

Appendix A

A.1

$$E_{11}(\kappa_1) = C_1 A \kappa_1{}^{-p} \quad (1A)$$

$$E(\kappa) = \frac{1}{2}\kappa^3 \frac{d}{d\kappa}\left(\frac{1}{\kappa}\frac{dE_{11}(\kappa)}{d\kappa}\right) \quad (2A)$$

Substitute (1A) into (2A)

$$E(\kappa) = \frac{1}{2}\kappa^3 \frac{d}{d\kappa}\left(\frac{1}{\kappa}\frac{d(C_1 A \kappa^{-p})}{d\kappa}\right)$$

$$E(\kappa) = \frac{1}{2}\kappa^3 \frac{d}{d\kappa}\left(-\frac{1}{\kappa}C_1 A p \kappa^{-p-1}\right)$$

$$E(\kappa) = \frac{1}{2}\kappa^3 \frac{d}{d\kappa}(-C_1 A p \kappa^{-p-2})$$

$$E(\kappa) = \frac{1}{2}\kappa^3 (p+2) p C_1 A \kappa^{-p-3}$$

$$E(\kappa) = \underbrace{\frac{1}{2}(p+2)pC_1}_{\boxed{C}} A \kappa^{-p}$$

$$C = \frac{1}{2}(p+2)pC_1$$

$$E(\kappa) = CA\kappa^{-p}$$

A.2

$$E_{22}(\kappa_1) = E_{33}(\kappa_1) = \frac{1}{2}\left(E_{11}(\kappa_1) - \kappa_1 \frac{dE_{11}(\kappa_1)}{d\kappa_1}\right) \quad (3A)$$

Substituting Eq. (1A) into (3A) ($\kappa = \kappa_1$)

$$E_{22}(\kappa) = \frac{1}{2}(C_1 A\kappa^{-p} + \kappa C_1 Ap\kappa^{-p-1})$$

$$E_{22}(\kappa) = \frac{1}{2}(C_1 A\kappa^{-p} + C_1 Ap\kappa^{-p})$$

$$E_{22}(\kappa) = \underbrace{\frac{1}{2}C_1(1+p)}_{\boxed{C_1{}'}}A\kappa^{-p}$$

$$E_{22}(\kappa) = C_1{}'A\kappa^{-p}$$

$$C_1{}' = \frac{1}{2}(1+p)C_1$$

A.3 Method 4: Energy spectrum from Fourier Transform of the time auto-correlation coefficient $\boldsymbol{R_E(\tau)}$ using property of convolution integral

Definitions

1. Definition of ω':

$$\omega' = 2\pi\omega$$

   Where ω' rad/s and ω hz and $d\omega' = 2\pi d\omega$

2. Given a function $f(t)$, its Fourier transform is

$$\hat{f}(\omega) = \int_{-\infty}^{\infty} f(t)e^{-i2\pi\omega t}\, dt = \int_{-\infty}^{\infty} f(t)e^{-i\omega' t}\, dt$$

And its inverse Fourier transform is

$$f(t) = \int_{-\infty}^{\infty} \hat{f}(\omega)e^{i2\pi\omega t}\, d\omega = \int_{-\infty}^{\infty} \hat{f}(\omega)e^{i\omega' t}\, d\omega$$

3. Given a function $f(t)$, the Fourier transform of its complex conjugate $f^*(t)$ is

$$\hat{f}^*(\omega) = \int_{-\infty}^{\infty} f^*(t)e^{i2\pi\omega t}\, dt = \int_{-\infty}^{\infty} f^*(t)e^{i\omega' t}\, dt$$

4. Given two functions $f(t)$ and $g(t)$ their convolution is defined by

$$h(t) = \int_{-\infty}^{\infty} f(t-s)g(s)ds \qquad \text{Pope D.14}$$

Or equivalently

$$h(t) = \int_{-\infty}^{\infty} f(s-t)g(s)ds$$

Proof at the end of the document

5. The time average of a function $f(t)$ over a time interval T is defined as

$$\overline{f} = \frac{1}{T}\int_{-T/2}^{T/2} f(t)dt$$

Or equivalently

$$\overline{f} = \frac{1}{2T}\int_{-T}^{T} f(t)dt$$

J.O. Hinze, Turbulence, page 62

6. Definition of the temporal auto correlation coefficient $R_E(\tau)$

$$R_E(\tau) = \frac{\overline{u(t)u(t+\tau)}}{\overline{u^2}}$$

7. Definition of the Fourier transform pair for $R_E(\tau)$ and $u(t)$

$$\mathcal{F}\{u(t)\} = \hat{u}(\omega) = \int_{-\infty}^{\infty} u(t)e^{-i\omega' t}dt \quad [m]$$

$$\mathcal{F}^{-1}\{\hat{u}(\omega)\} = u(t) = \int_{-\infty}^{\infty} \hat{u}(\omega)e^{i\omega' t}d\omega \ \ [m/s]$$

$$\mathcal{F}\{R_E(\tau)\} = \hat{R}_E(\omega') = \int_{-\infty}^{\infty} R_E(\tau)\, e^{-i\omega'\tau}d\tau \quad [s]$$

$$\mathcal{F}^{-1}\{\hat{R}_E(\omega')\} = R_E(\tau) = \frac{1}{2\pi}\int_{-\infty}^{\infty} \hat{R}_E(\omega')\, e^{i\omega'\tau}d\omega' \quad [-]$$

Proof:

$$h(t) = \int_{-\infty}^{\infty} f(t-s)g(s)ds = \int_{-\infty}^{\infty} f(s-t)g(s)ds$$

Let $u = t - s$, then $du = -ds$ and when $s = -\infty$, $u = \infty$, and when $s = \infty$, $u = -\infty$. Substituting this in the first integral, we get:

$$\int_{-\infty}^{\infty} f(t-s)g(s)ds = -\int_{\infty}^{-\infty} f(u)g(t-u)du$$

Now, we can use another change of variables in the second integral.

Let $v = t - u$. Then, $dv = -du$, and when $u = -\infty$, $v = \infty$, and when $u = \infty$, $v = -\infty$. Substituting this in the second integral, we get:

$$-\int_{\infty}^{-\infty} f(u)g(t-u)du = \int_{-\infty}^{\infty} f(t-v)g(v)dv$$

Notice that the limits of integration in the second integral are reversed. We can reverse them by changing the sign of the integral:

$$\int_{-\infty}^{\infty} f(t-v)g(v)dv = -\int_{\infty}^{-\infty} f(t-v)g(v)(-dv)$$

Then, changing the variable of integration back to s, we get:

$$-\int_{\infty}^{-\infty} f(t-v)g(v)(-dv) = \int_{-\infty}^{\infty} f(s-t)g(s)(ds)$$

Therefore, we have shown that

$$\int_{-\infty}^{\infty} f(t-s)g(s)ds = \int_{-\infty}^{\infty} f(s-t)g(s)ds$$